

Operational Dynamic Response of Burj Khalifa and Reinforced Concrete Buildings for Safety Against Pounding

Praveena Rao* and Hemaraju Pollayi

Department of Civil Engineering, GITAM University, Hyderabad-502329, Telangana State, India

* Corresponding author. E-mail: raopraveena6@gmail.com DOI: 10.14416/j.asep.2023.01.006

Received: 14 October 2022; Revised: 25 November 2022; Accepted: 23 December 2022; Published online: 18 January 2023

© 2023 King Mongkut's University of Technology North Bangkok. All Rights Reserved.

Abstract

Random ground motions in horizontal, vertical and arbitrary directions radiate away from the focus or the hypocenter under the surface of the earth during an earthquake. When the earth shakes violently, the buildings, which act as vertical cantilevers, undergo vibrations inducing significant inertial forces. Large uncertainties are associated with the response of the buildings to random lateral forces; thus it is of paramount importance to understand the dynamic structural behavior of high rise buildings. Real world high rise building such as Burj Khalifa has been analyzed by response spectrum analysis with the lumped-mass model. The response of Burj Khalifa is simulated when subjected to ground acceleration motion of different earthquake recordings within a MATLAB framework. The ground motion acceleration databases of the El Centro earthquake in 1940 and Bhuj earthquake in 2001 are taken as inputs for the present analysis with other inputs pertaining to different storey masses, storey-stiffness, number of stories, damping ratios and mode shapes. Furthermore, numerical examples to demonstrate the impact of a safe seismic gap between adjacent buildings to prevent pounding or collision during seismic events are presented. It may be observed that computation and adoption of critical gaps between buildings facilitate the best-optimized use of land and provide safety against the pounding of multi-storey buildings under the effect of earthquake excitations.

Keywords: Dynamic analysis, Burj Khalifa, Modal analysis, Peak displacement, Structural pounding, Seismic gaps

1 Introduction

The present work exemplifies the behavior of multi-degrees-of-freedom (MDOF) systems subjected to dynamic earthquake loads Response Spectrum Method using Newmark's time integration operators for MDOF linear systems. Dynamic analysis is categorized into linear and nonlinear approaches for estimating the dynamic response of structures. The linear approach involves the response spectrum method and time history modal analysis of structures subjected to loads of dynamic nature, such as earthquake ground motion, lateral wind loads, heavy traffic and blasting forces [1]. Waghmare *et al.* [2] have performed a response spectrum analysis of multi degrees of freedom structure using MATLAB. For the seismic

analysis of multi-degree-of-freedom structures, a state-space representation was formulated by Ali *et al.*, and linear time history analysis is implemented for the analysis of large configuration structures, which are subjected to El Centro earthquake excitation forces [3]. Yadav [4] analyzed two different buildings of irregular configurations with time history analysis using ETABS. Seismic loadings from different time zones were subjected to test buildings in a case study of a 19-storey building. A lumped mass system is assumed and a modal participation factor is computed with modal analysis to determine the shear forces. SRSS (Square-Root-of-Sum-of-Squares) combination rule has been used to approximate maximum modal story displacement [5], [6].

The fundamental objective of the seismic analysis



is to design earthquake resistant buildings, which are capable of withstanding the effects of violent shaking, resisting swinging or collapsing, and preventing loss of life and property. With the advent of high power computational software applications and numerical analysis techniques, the behavior of single degree of freedom (SDOF) and MDOF structures of different configurations can be analyzed with the modal superposition of input parameters, such as mass, ground motion acceleration data sets, damping coefficient, stiffness and mode shapes [7], [8]. Friuli earthquake and Petrolia earthquake time history data are subjected to building models with 6×5 bay up to 10 floors in the edge position and 2×2 bay up to the top floor in the center position. The ground motion record of the El Centro earthquake (1940), Imperial County, California was the first completely recorded earthquake in the history of structural dynamics studies. Hence, the most studied earthquake with a magnitude of 6.9 Mw and acceleration of 3.41 m/s^2 has been taken as a benchmark in the present analysis for verification. The ground motion data of the Bhuj earthquake, 26 January 2001, Gujarat with a magnitude of 7.8 Mw and recorded peak ground acceleration of -1.0382 m/s^2 is used in the present work. High seismic activities of greater intensities are witnessed around the regions of Kutch in the state of Gujarat and the northeastern states of India [9]. Based on the past 50 year earthquake records, these regions are listed in Zone V indicative of very high-risk seismic zones in the country.

In the present times, multi-storey building frames are the most common constructions taking place in the urban settlements catering to the needs of affordable housing and lack of space for large metropolitan populations. Thus, seismic provisions are incorporated in the design and planning stage such that the buildings are capable of undergoing minor earthquake shaking without any damage to the structure. Also, withstand moderate earthquakes by sustaining minor non-structural damages and avert collapsing of buildings during severe earthquake events [10]. The behavior of buildings is largely dependent on the distribution of stresses along different planes when subjected to several types of static and dynamic forces during their lifetime [11], [12]. It was reported that the first mode shape or the fundamental mode had the maximum influence on the response of the structure. 86.96% of the mass responds to the ground excitation motion

in the first mode and 8.91% responds in the second mode. Thus, the mass of the MDOF system responds significantly in the first two mode shapes. The overall mode shapes depend upon some factors that influence the behavior of the building, such as geometrical configurations, properties and quality of materials used for structural members, lateral distribution of storey stiffness along with the height of building and foundation level connections with structural members. Several composites and environment friendly materials are being used presently in the building construction industry [13], which influence the building characteristics and seismic behavior of the structures greatly. Maximum acceleration, velocity and displacements are computed and the results of the model are compared with the traditional methods. Chhindam and Autade [14] analyzed setback and mass irregularities in two building models by defining all material and dimensional properties. Displacement, equivalent lateral forces, base shear and stresses are computed and validated for the analysis. It was concluded that buildings with vertical irregularities showed better performance than regular buildings. Thus, proper design and detailing for adequate strength, stability and serviceability are of paramount importance.

Ground acceleration \ddot{X}_g is used as the input signal for the analysis of a five-storey shear frame with a storey height of 4 m by the developed mathematical model [15]. Ricke [16] has performed the dynamic analysis of structures using Python v3.7 of buildings in the response spectrum method as per the Indian standard codes for seismic analysis (IS 1893 (Part-1): 2002). A nine-storey frame building with a 6×3.75 m span in x -directions and y -directions, respectively, is considered for analysis with the response spectrum method using Python and ETABS. The natural frequency, modal mass, modal participation factors, shear forces and displacement results of modal analysis by response spectrum analysis with ETABS, Python and manual computations are compared and plotted. The ground acceleration time-history data of the Bhuj earthquake, Koyna earthquake, Anza earthquake, Nahanni earthquake and Northridge earthquake are taken for the dynamic analysis. George [17] analyzed the structural response of the MDOF system with response spectrum analysis by programming algorithms for different spectra. They analyzed and compared

the results of acceleration, velocity and displacement spectra using 11 strong ground motion databases with different software applications. The seismic response of a ten storey MDOF building is modeled and analyzed using SAP2000-15 software for different seismic intensities. The seismic behavior of the considered RCC buildings is compared for different earthquake intensities in Modified Mercalli's Intensity scale. Seismic responses comprising base shears, storey displacements and storey drifts are computed for earthquake intensities ranging from V-X (MMI scale) [18]. Latifi [19] has developed a numerical model for seismic analysis of structures by response spectrum analysis conforming to Eurocode 8 provisions. A five-storey moment-resisting 3D structure is subjected to ground motion and analyzed with eigenvector analysis for undamped free vibrations. The lumped mass matrix and stiffness matrix are used to compute vibration mode shapes and natural frequencies of the structure. Using the Newmark's Method for linear systems the author has developed a response spectra model for numerical analysis of MDOF systems in MATLAB [20]. The ground acceleration time series data, and structural parameters including mass, stiffness, and damping ratio are taken as inputs in the developed model for different mode shapes [21], [22]. Freeman has studied the response of structures with the linear response spectrum method and nonlinear pushover analysis [23]. The absolute displacements, base shear forces and story drifts of multi-storey buildings as per the Eurocodes provisions. An eight-storey building is analyzed and results of both linear response spectrum analysis and nonlinear static pushover analysis are compared. The simulation of the modeled structure is performed in force RPA99/version 2003 and ETABS 2013 program as per the Algerian seismic design code guidelines.

The computation of the critical distance between two adjacent buildings prone to collision or pounding when subjected to earthquake excitations is of paramount importance [24]. The authors have numerically analyzed a five-storey building with different masses ranging from 15000kg to 55000kg and varying stiffness from 0.1×10^6 N/m to 5×10^6 N/m subjected to six earthquake ground motion records [25], [26]. The impact of pounding between two adjacent systems is numerically simulated for the peak values of lateral displacement and impact forces considering the stiffness [27]–[30]. Khatami *et al.* have modeled SDOF

structures with 5% damping and established four different calculation criteria for adequate separation between adjacent buildings [31]–[35]. SDOF systems are considered for a parametric study of visco-elastic nonlinear models.

2 Analytical Formulation

2.1 MDOF equations of motion

The time history analysis and response spectrum method are the most commonly used methods for evaluating the dynamic response of structures. Reinforced concrete buildings with n degrees of freedom (DOF) subjected to earthquake excitations are idealized as lumped-mass systems where the total mass is assumed to be concentrated at the floor levels for developing a mathematical model [36]. The dynamic response of MDOF structures can be determined with the combination of different mode shapes, modal natural frequency and modal mass. Earthquake-resistant design concept ensures a balance between damage within acceptable limits and reduced cost of construction for a viable project design. Based on post-earthquake damage assessment and upon extensive research, engineers and architects aim to design structures with adequate lateral strength, stiffness and ductility to accommodate lateral deformations. The response spectrum is a plot of the maximum response of linear single degrees of freedom system oscillators when subjected to earthquake excitations and its natural frequency or time period for a given damping [37]. It helps in obtaining the peak values or maxima of the structural response comprising displacement, velocity and acceleration response. The response spectrum method is of great importance for engineering purposes, as it gives crucial information pertaining to maximum forces and maximum displacement for which the structure must be designed. The total combined response of different modes for multi-story buildings with symmetric plans is estimated with Newmark's method for numerical integration as in Equations (1)–(7). The equation of motion for MDOF structures with different modes of vibrations or mode shapes is given as:

$$m\ddot{u} + c\dot{u} + ku = -m\ddot{u}_g(t) \quad (1)$$

where, m is mass matrix, c is damping matrix, k is

stiffness matrix, $\ddot{u}g(t)$ is ground motion acceleration and i is influence vector. The natural frequencies and natural modes of vibration are determined by the following equations:

$$\{[K] - \omega_i^2[M]\} \{\phi_i\} = 0 \quad (2)$$

where:

ω_i^2 is eigen value of the i^{th} mode,

ϕ_i is the eigen vector or mode shape of the i^{th} mode,

ω_i is the natural frequency in the i^{th} mode, and $i = 1, 2, \dots, n$ and n is the number of DOFs. The floor displacement, storey drifts and base shears are computed as given below;

$$u_{jn} = \Gamma_n \phi_{jn} D_n \quad (3)$$

$$\Delta_{jn} = \Gamma_n (\phi_{jn} - \phi_{j-1,n}) D_n \quad (4)$$

Base shear V_{bn} is computed as;

$$V_{bn} = M_n \times A_n \quad (5)$$

The peak response for equivalent static forces for n^{th} mode is:

$$f_n = s_n \times A_n \quad (6)$$

where, f_n is a force vector of f_{jn} at varying floor levels $j = 1, 2, 3, \dots, N$.

$$f_{jn} = \Gamma_n m_j \phi_{jn} A_n \quad (7)$$

Thus, the response of each mode shape can be computed as a function of time and the total response of MDOF structures can be determined by the summation of modal responses. The combined effect of all modal responses by modal superposition gives the response of structures subjected to earthquake excitations. Every mode has a particular deformation pattern, mode shape and natural frequency. The influence of the first few modes dominates the overall response and the deformed shape associated with the fundamental time period is known as the first mode shape of oscillation.

2.2 Seismic gap for safety against pounding

Structural pounding is the phenomenon, which results

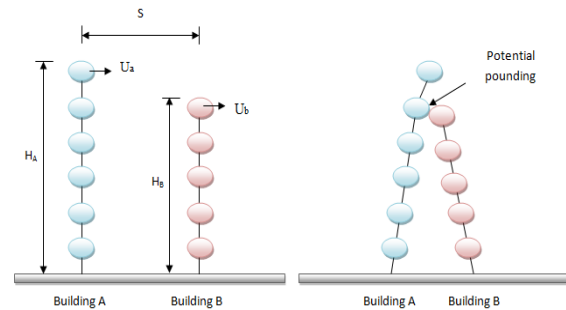


Figure 1: Analytical collision model of (a) Adjacent buildings at rest position and (b) Adjacent buildings during seismic pounding.

in collision of adjacent MDOF buildings during earthquakes due to inadequate seismic gap or critical separation distance between buildings. Consequently, lateral displacements are larger than the critical gap and relative movements of the buildings in-between result in severe damages due to pounding. The separation distance for safety against pounding has been computed mathematically by several authors conforming to different country codes and requirements as given in Equations (8)–(10). The building codes of most countries follow the Absolute Sum method (ABS) and Square-Root-of-Sum-of-Squares (SRSS), given by the following equations:

$$S = \delta_i + \delta_j \quad (8)$$

$$S = \sqrt{\delta_i^2 + \delta_j^2} \quad (9)$$

where, S is the seismic gap provided between buildings, δ_i and δ_j are the maximum lateral displacements of two adjacent buildings i and j , respectively. Some other country codes have adopted the height of the buildings for determining the separation distance given by the following equation:

$$S = 0.05 (h_i + h_j) \quad (10)$$

where, h_i and h_j are the heights corresponding to two adjacent buildings i and j as shown in Figure 1.

Seismic gap for adjacent buildings recommended by other country codes are:

1) Indian Standard Codes: The separation between two adjacent buildings or units shall be computed as stated in Clause 7.11.3 given by R times the sum

of peak displacements of structures, where R is the response reduction factor to be adopted from the values given in Table 7, IS1893 [38]–[40].

2) Canadian Building Codes: The safe distance for seismic separation between MDOF buildings shall be computed as the summation of peak displacements of individual buildings subjected to lateral earthquake forces for elastic systems.

3) Australian Building Codes: The seismic gap provided shall be greater than 1% of the height of any multi-storey structure.

4) Egyptian Codes: The safe distance is determined as twice the summation of maximum displacements of structures or 0.004 times the height of the building.

Several authors have worked on the computation of safe seismic gap to prevent the pounding of buildings and can be derived by the following Equations (11)–(16):

$$S = \sqrt{\delta_i^2 + \delta_j^2 - 2\rho_{op}\delta_i\delta_j} \tag{11}$$

where ρ_{op} is called the cross-correlation coefficient and give by the following equation:

$$\rho_{op} = \frac{8\sqrt{\zeta_i\zeta_j} \left[\zeta_i + \zeta_j \left(\frac{T_i}{T_j} \right) \right] \left(\frac{T_i}{T_j} \right)^{1.5}}{\left[1 - \left(\frac{T_i}{T_j} \right)^2 \right]^2 + 4\zeta_i\zeta_j \left[1 - \left(\frac{T_i}{T_j} \right) \right] \left(\frac{T_i}{T_j} \right) + 4(\zeta_i^2 + \zeta_j^2) \left(\frac{T_i}{T_j} \right)^2} \tag{12}$$

where T_i and T_j taken are the vibration periods and ζ_i and ζ_j are the damping ratios of adjacent buildings i and j . Further, the following equations were derived by Penzien [27] for a building i with nonlinear vibration period T_{i-non} and damping ratios ζ_{i-non} as given below:

$$T_{i-non} = T_i \sqrt{\phi_i} \tag{13}$$

$$\zeta_{i-non} = \zeta_i + \omega_i \tag{14}$$

where ϕ_i and ω_i can be given by the following equations:

$$\phi_i = \frac{\mu_i}{\gamma + \alpha_i(\mu_i - \gamma)} \tag{15}$$

$$\omega_i = \frac{2(\mu_i - \gamma)(1 - \alpha_i)}{\pi \mu_i(\gamma + \alpha_i(\mu_i - \gamma))} \tag{16}$$



Figure 2: Burj Khalifa, Dubai [41].

where μ_i is called displacement ductility, γ is a constant value considered to be equal to 0.65, and another term called α_i is the ratio between ultimate stiffness with its initial value.

3 Numerical Examples

3.1 Modal analysis of Burj Khalifa

Burj Khalifa, Dubai the tallest structure in the world with 828 m height and 162 floors is integrated with advanced architectural structural systems shown in Figure 2. Complex architectural design and engineering concepts by Skidmore, Owings and Merrill were developed with the help of advanced structural analysis and design software tools considering minimum code requirements shown in Figure 3. The total floor area of 460,000 m² consists of luxury hotels, residential units, commercial spaces, offices, shopping and entertainment complexes [41]. The building design pattern is inspired by an indigenous desert flower with a central hexagonal core or tower massing with three wings forming a Y-shaped cross-section as shown in Figure 4.

Aerodynamic shaping and high-frequency dynamic wind analysis play a major role in determining

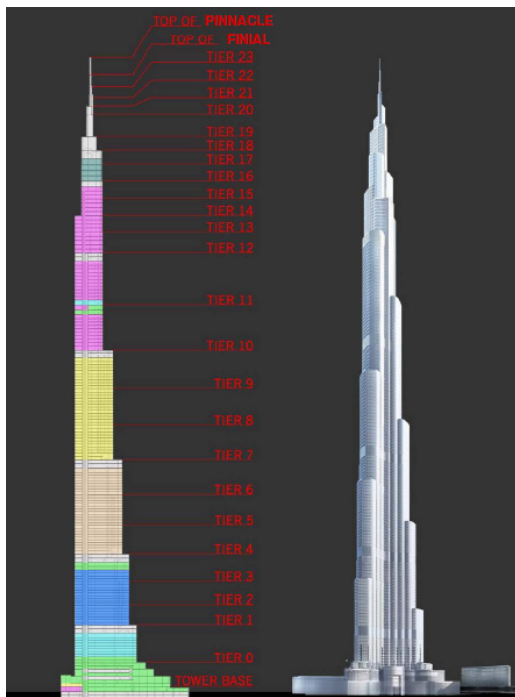


Figure 3: Burj Khalifa tower tiers and plan [43].

the structural behavior of the tower and mitigating the effects of dynamic lateral forces [42]. About 40 wind tunnel tests were performed to compute the net wind loads acting on the structure as increased height is a critical factor. Aerodynamic shaping is essential for designing an appropriate geometric shape, which improves the behavior of the structure subjected to dynamic winds acting at such heights. Thus, the response of Burj Khalifa tower was controlled greatly by the reduction of wind forces with the implementation of effective wind engineering techniques resulting in the tapered geometry of the tower [43].

The superstructure is constructed with high performance reinforced concrete and steel frame bracing system provided beyond the 156th floor to the top of the tower. The vertical structural members were constructed with high performance grades of concrete C60–C80, while the horizontal members were built with C50 concrete grade [44]. The exterior facade of the tower is paneled with lightweight curtain walls of glass and different metals such as aluminium and stainless steel. These curtain walls are of reflective texture to cater to the need for thermal protection against excessive solar radiation and extreme weather conditions in

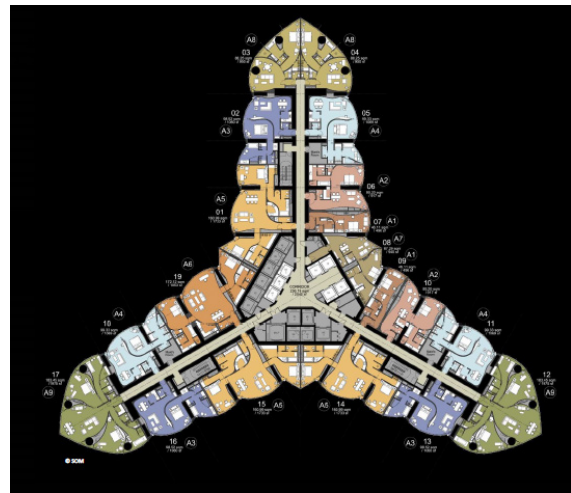


Figure 4: Typical floor plan of Burj Khalifa [43].

the desert city [45]. State-of-art technologies were implemented for achieving greater accuracy in the construction and maintenance of the structure. For the structural health monitoring of the structure, real-time measurement of building accelerations and displacements at different floors due to lateral wind and seismic loads is of paramount importance [46]. In this section, response spectrum analysis of the tallest tower structure is attempted by considering the available data for its design parameters.

In the present work, extensive databases are generated for earthquake recordings taken as inputs, which include El Centro earthquake, N-S component with 6.9 Mw intensity and Bhuj earthquake, N 78 E component with 7.8 Mw intensity. These accelerograph data are taken from COSMOS strong motion virtual data center portal. The El Centro earthquake (Imperial County, California), in 1940, for which the data set is generated consists of 1,559 data points of recorded ground motion acceleration at 0.02 s time-intervals. Bhuj earthquake, in 2001, dataset consists of 26,706 ground motion acceleration data points recorded at 0.005 s intervals. These databases are used as inputs to perform seismic analysis of structure with response spectrum analysis using the modal superposition rules for MDOF structures. The floor-wise mass, stiffness and damping ratio of 2% are also considered as inputs. The El Centro earthquake excitation is used as a benchmark for the analysis. Any structure can have infinite degrees of freedom, which are reduced to finite

depending on the numbers of floors in the structure for analysis. The fundamental mode of oscillation is considered the mode shape with the smallest natural frequency [47].

3.2 Burj Khalifa design parameters

For performing the seismic response spectrum analysis of Burj Khalifa, the storey masses and stiffness of the tower are approximately computed considering the following data as given in Table 1. The total quantities of materials used in the construction have been computed to estimate the total mass of the tower. The data available regarding the floor area of different stories have been considered for the approximate calculation of the storey masses, as the exact data pertaining to storey masses and stiffness has not been given by the Burj Khalifa authorities. Thus, the total mass of the tower has been distributed to each floor according to their corresponding floor areas. The ratio of floor area (*a*) at each storey to the total floor area (*A*) of the tower has been termed as an area-wise non-dimensional parameter and can be given as in Equation (17):

$$\text{Area-wise non-dimensional parameter} = \frac{a}{A} \quad (17)$$

Thus, the mass at each floor (*m*) can be calculated as:

$$m = \frac{a}{A} M \quad (18)$$

where *M* is the total mass of Burj Khalifa tower and is given by the following equation:

$$M = \text{Mass of concrete} + \text{Mass of steel reinforcement} + \text{Mass of glass} + \text{Mass of aluminium} \quad (19)$$

From the data given below in Table 1, the total mass of concrete, the mass of steel reinforcement, the mass of glass used for curtain walls and the mass of other metals used including aluminium and stainless steel have been computed. The density of materials is taken as 2500 kg/m³ for concrete, 2500 kg/m³ for glass, 2700 kg/m³ for aluminium and 7500 kg/m³ for stainless steel used in the cladding of glass panel. The total mass *M* of Burj Khalifa tower summed up to 948,330,000 kg and the storey masses (*m*) were computed as per Equations (18) and (19).

Table 1: Estimation of materials used for construction

S.No.	Materials	Quantities
1	Total concrete	330,000 m ³
2	Total steel rebars	39,000 t
3	Total glass used for facade	103,000 m ²
4	Total stainless steel used for cladding	15,500 m ²
5	Total aluminium used for cladding	27,900 m ²

Further, the storey stiffness was computed by equations of simple harmonic motion. The time period (*T*) of the tower was determined by a dynamic analysis performed during the construction stage [42] as shown in Figure 5. The values of (*T*) were found to be as given below in Table 2:

Table 2: The time period (*T*) values

T	Time Period Value
T ^{1st Mode}	11.3 s for the fundamental mode of vibration
T ^{2nd Mode}	10.2 s for 2nd mode laterally perpendicular sway
T ^{5th Mode}	4.3 s for 5th mode torsional motion

The mode shapes obtained by MATLAB simulations of Burj Khalifa [48] when subjected to benchmark El Centro ground motion acceleration with the above-computed storey masses and stiffness are shown. The area-wise non-dimensional parameter calculated for the computation of storey masses is summarized in Table 3. The dynamic analysis of Burj Khalifa is performed with modeled structure as given above for different mode shapes while considering 0, 1, and 2% damping, respectively, as shown in Figures 6–8. It may be observed that the floor-area ratio is less at the 41st, 74th, 110th and 137th-floor levels thus, having less mass and stiffness at corresponding floor levels. Maximum roof displacement is found on the 160th floor of Burj Khalifa for 0, 1, and 2% damping and is observed to be 0.33440 m, 0.33437 m, and 0.33434 m, respectively in the fundamental mode of vibration.

3.3 Structural pounding

For studying the behavior of structural pounding in between adjacent buildings, a five-storey lumped-mass model was considered with different mass and storey stiffness. Linear elastic response spectrum analysis was performed to assess the behavior of different building models subjected to El Centro earthquake, Bhuj earthquake and India-Myanmar earthquake ground

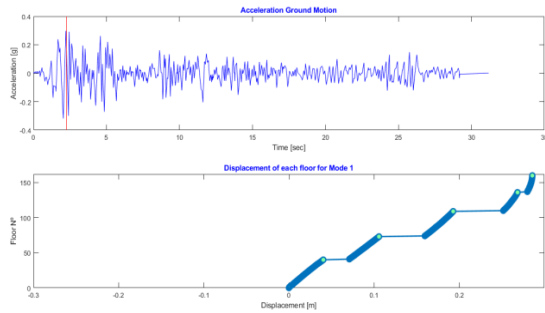


Figure 6: Burj Khalifa tower peak displacement for mode shape 1 with no damping.

motion accelerations. Peak lateral displacements for the different building models can be studied from the plots shown in Figures 9 and 10.

Table 3: Storey-wise floor-area ratios in Burj Khalifa

Floor No.	Floor Area (a) (sq.ft.)	a/A	m(kg)	k(N/m)
1	91482	0.02811451	26661833.01	8249780.43
2	32219	0.009901635	9390017.683	2905486.06
3	48976	0.015051444	14273736.18	4416620.17
4	21862	0.006718692	6371537.496	1971499.31
5-6	38363	0.011789827	11180646.46	3459547.53
7-18	33607	0.010328199	9794541.242	3030654.89
19-25	31962	0.009822653	9315116.707	2882309.99
26-33	30318	0.009317414	8835983.616	2734055.26
34-37	26673	0.008197223	7773672.109	2405351.80
38-40	28673	0.008811868	8356559.081	2585710.35
41	1000	0.000307323	291443.4862	90179.2749
42	28673	0.008811868	8356559.081	2585710.35
43-52	26845	0.008250082	7823800.388	2420862.64
53-63	25017	0.007688296	7291041.695	2256014.92
64-73	23189	0.00712651	6758283.003	2091167.21
74	438	0.000134607	127652.247	39498.5224
75	23189	0.00712651	6758283.003	2091167.21
76-86	20873	0.00641475	6083299.888	1882312.01
87-98	18557	0.00570299	5408316.774	1673456.81
99-109	16241	0.004991231	4733333.66	1464601.61
110	207	6.36158E-05	60328.80165	18667.11
111	16241	0.004991231	4733333.66	1464601.61
112-123	13515	0.004153468	3938858.717	1218772.90
124-136	10788	0.003315399	3144092.33	972854.018
137	344	0.000105719	100256.5593	31021.67
138	10788	0.003315399	3144092.33	972854.018
139-140	7609	0.00233842	2217593.487	686174.10
141-143	8061	0.00247733	2349325.943	726935.14
144-147	7044	0.002164782	2052927.917	635222.81
148-151	6026	0.001851928	1756238.448	543420.31
152-155	5008	0.001539073	1459548.979	451617.81
156-158	4129	0.001268936	1203370.155	372350.23
159-160	3250	0.000998799	947191.3303	293082.64

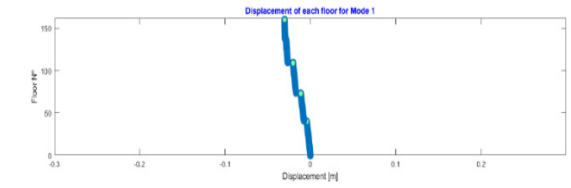


Figure 7: Burj Khalifa tower peak displacement for mode shape 1 with 1% damping.

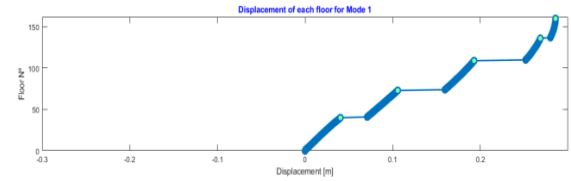


Figure 8: Burj Khalifa tower peak displacement for mode shape 1 with 2% damping.

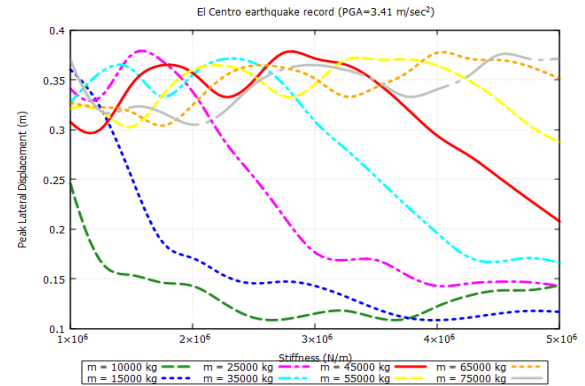


Figure 9: Peak lateral displacements for buildings with different mass and stiffness models subjected to EL Centro ground motion.

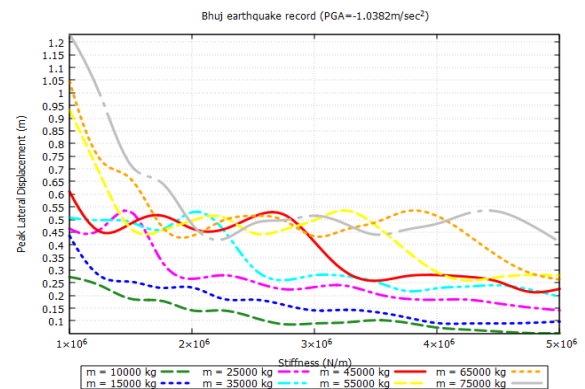


Figure 10: Peak lateral displacements for buildings with different mass and stiffness models subjected to Bhuj earthquake ground motion.

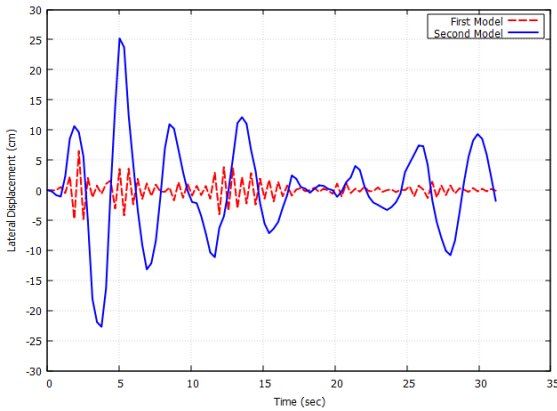


Figure 11: Lateral displacement time histories of adjacent building models without seismic gap.

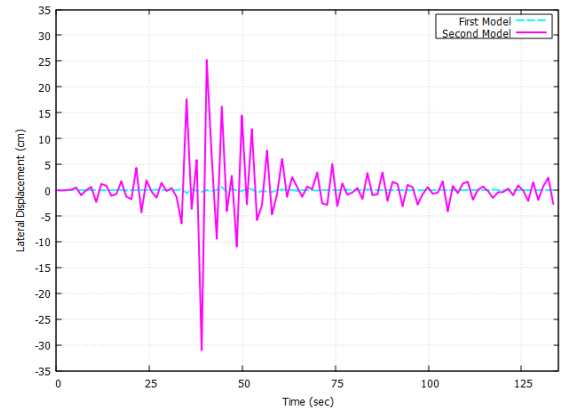


Figure 13: Lateral displacement time histories of adjacent building models without a seismic gap.

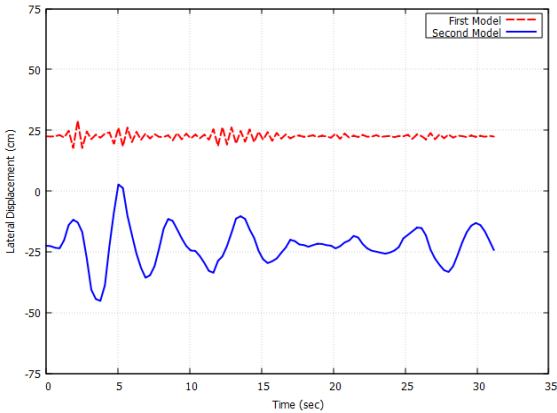


Figure 12: Lateral displacement time histories of adjacent building models with safe seismic gap of 44.9925cm subjected to El Centro ground motion.

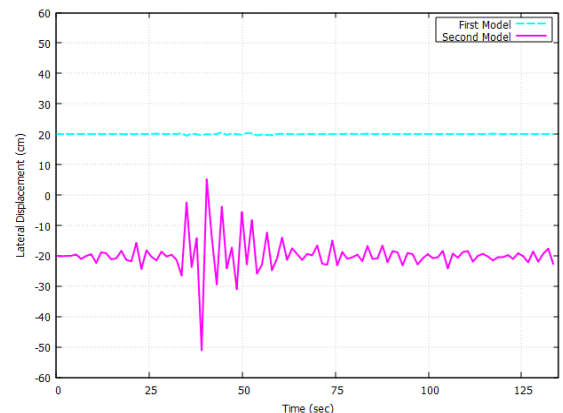


Figure 14: Lateral displacement time histories of adjacent building models with a safe seismic gap of 40.1207 cm subjected to Bhuj earthquake ground motion.

Storey masses of 10,000, 15,000, 25,000, 35,000, 45,000, 55,000, 65,000, and 75,000 kg have been adopted for different building models with stiffness ranging from 1×10^6 N/m to 5×10^6 N/m and 5% damping ratio. The safe seismic gap or critical distance to be provided between adjacent multi-storey buildings is computed as per Equation (25) for two building models considered as Model 1 and Model 2 as shown in Figures 11 and 12.

Model 1 is a six-storey MDOF structure taken from section 3.1, whereas, Model 2 is a five-storey MDOF structure with storey masses 15,000, 25,000, 35,000, 45,000, and 55,000 kg and storey stiffness 0.89×10^6 , 1.45×10^6 , 2×10^6 , 2.6×10^6 , and 3.15×10^6 N/m. Lateral displacements of the two model buildings are

determined by the response spectrum method and lateral displacement time history plots are generated.

Figure 11 illustrates the impact of structural pounding when a safe critical gap is not provided between two adjacent buildings. The lateral displacement time history of both building models with a safe seismic gap of 44.9925 cm when subjected to El Centro ground motion as shown in Figure 12.

Similarly, the effects of structural pounding on adjacent buildings subjected to Bhuj earthquake motion without a seismic gap can be observed in Figure 13. The lateral displacement time history of building models 1 and 2 with a safe critical distance of 40.1207 cm, when subjected to Bhuj earthquake ground excitation, can be observed in Figure 14.



4 Conclusions

This paper deals with the dynamic analysis of multi-storey reinforced concrete buildings subjected to ground excitations. During earthquakes, strong ground motion waves radiate from the hypocentre in random directions, which on reaching the base of buildings induces back-and-forth oscillatory motion. Numerical examples are presented with MATLAB simulations for analyzing the response of Burj Khalifa with the response spectrum method. The building properties including mass, stiffness and damping ratios are also taken as input parameters. Burj Khalifa, the tallest structure is designed with complex architectural and engineering concepts. Seismic response spectrum analysis of Burj Khalifa is performed where the storey masses and stiffness of the tower are approximately computed based on floor-area ratios. The total mass of the tower has been distributed to each floor and corresponding stiffness values are computed for 160 floors. Maximum displacement of the Burj Khalifa model structure considering 0, 1, and 2% damping was found to be 0.33440, 0.33437, and 0.33434 m, respectively in the fundamental mode of vibration. The second part of this work is focused on the critical distance between two adjacent buildings to prevent pounding during earthquake excitations. Two building frames of five and six stories with different masses and stiffness are considered to demonstrate the effects of structural pounding. The safe seismic gap or critical distance computed for the two building models was found to be 44.9925 cm and 40.1207 cm for El Centro and Bhuj earthquake ground motions, respectively. It may be stated that with the provision of a safe critical gap between adjacent buildings pounding of structures can be prevented during severe earthquake events.

Acknowledgments

This research did not receive any specific grant from any funding agencies in the public, commercial, or not-for-profit sectors.

Author Contributions

P.R.: conceptualization, investigation, reviewing and editing; methodology, data analysis, data curation, writing an original draft; H.P.: research design, data

analysis, data curation, conceptualization, reviewing and editing. All authors have read and agreed to the published version of the manuscript.

Conflicts of Interest

The authors declare no conflict of interest.

References

- [1] G. M. Calvi, M. J. N. Priestley, and M. J. Kowalsky, "Displacement-based seismic design of structures," presented at 3rd Panhellenic Antiseismic Conference Engineering and Technical Seismology, Athens, Greece, Nov. 5–7, 2008.
- [2] P. B. Waghmare, P. S. Pajgade, and N. M. Kanhe, "Response spectrum analysis of a shear frame structure by using MATLAB," *International Journal of Applied Science and Engineering Research*, vol. 1, no. 2, pp. 1–10, 2012.
- [3] B. H. Ali, B. A. Saeed, and T. A. Hussein, "Time history analysis of frame structure systems by state-space representation method," *Polytechnic Journal*, vol. 10, no. 1, pp. 140–147, 2020.
- [4] H. Yadav and A. Gupta, "Time history comparison of building structure using Etabs," *International Journal of Research*, vol. 5, no. 15, pp. 1720–1725, 2018.
- [5] A. B. M. S. Islam, S. I. Ahmad, and J. Mohammed, "Generation of response spectra along with time history for earthquake in Dhaka for dynamic analysis of structure," *SUST Studies*, vol. 14, no. 2, pp. 56–68, 2011.
- [6] A. S. Patil and N. P. D. Kumbhar, "Time history analysis of multistoried RCC buildings for different seismic intensities," *International Journal of Structural and Civil Engineering*, vol. 2, no. 3, pp. 194–201, 2013.
- [7] M. T. Raagavi and S. Sidhardhan, "A study on seismic performance of various irregular structures," *International Journal of Research in Engineering and Science*, vol. 9, no. 5, pp. 12–19, 2021.
- [8] S. K. Dubey, P. Sangamnerkar, and A. Agrawal, "Dynamics analysis of structures subjected to earthquake load," *International Journal of Advanced Engineering and Research*

- Development*, vol. 2, no. 9, pp. 11–19, 2015.
- [9] E. H. Susan, M. Stacey, B. Roger, and M. A. Gail, “The 26 January 2001 M 7.6 Bhuj, India, Earthquake: Observed and predicted ground motions,” *Bulletin of the Seismological Society of America*, vol. 92, no. 6, pp. 2061–2079, 2002.
- [10] K. S. Patil, S. S. Desai, R. S. Dahifale, T. P. Shashikant, and A. M. Rajput, “Time history analysis and design of multi-storeyed building,” *International Journal of Research in Engineering and Science*, vol. 9, no. 7, pp. 38–43, 2021.
- [11] F. D. Luca and L. Lombardi, “Ec8 design through linear time history analysis versus response spectrum analysis – Is it an enhancement for Pbee,” presented at 16th World Conference on Earthquake, Santiago, Chile, Jan. 9–13, 2017.
- [12] S. G. Dasari and K. S. Rao, “Seismic and time history performance of RCC framed buildings with and without passive energy dissipators,” *International Journal of Engineering and Advanced Technology*, vol. 9, no. 3, pp. 2230–2240, 2020.
- [13] M. Puttegowda, H. Pulikkalparambil, and S. M. Rangappa, “Trends and developments in natural fiber composites,” *Applied Science and Engineering Progress*, vol. 14, no. 4, pp. 543–552, 2021, doi: 10.14416/j.asep.2021.06.006
- [14] C. Chhindam and P. Autade, “Seismic time history analysis of six story shear building with newmark- β method and ETABS,” *International Journal of Research in Engineering and Technology*, vol. 7, no. 3, pp. 49–54, 2018.
- [15] N. Takahashi and Y. Hachiro, “Sequential time-history analysis of building structures under Earthquake and Tsunami Loads,” presented at Eleventh U. S. National Conference on Earthquake Engineering, Los Angeles, California, Jun. 25–29, 2018.
- [16] S. Ricke and B. K. R. Prasad, “Response spectrum analysis of tall building using python,” *International Journal of Engineering Research and Technology*, vol. 8, no. 7, pp. 1000–1006, 2019.
- [17] P. George and P. Vagelis, “Open seismo matlab: A new open-source software for strong ground motion data processing,” *Heliyon*, vol. 4, no. 9, 2018, Art. no. e00784.
- [18] J. Pengcheng and H. A. Amir, “Artificial intelligence in seismology: Advent, performance and future trends,” *Geoscience Frontiers*, vol. 11, no. 3, pp. 739–744, 2019.
- [19] L. Reza and R. Rahimeh, “Three-dimensional numerical model for seismic analysis of structures,” *Civil Engineering and Architecture*, vol. 8, no. 3, pp. 237–245, 2020.
- [20] R. Makara, “Seismic analysis: Response spectrum analysis method with MATLAB,” Gangneung-Wonju National University, Korea, 2016.
- [21] T. Mostafa, “Simulation of strong ground motion parameters of the 1 June 2013 Gulf of Suez Earthquake Egypt,” *NRIAG Journal of Astronomy and Geophysics*, vol. 6, no. 1, pp. 30–40, 2016.
- [22] J. P. McCalpin and M. G. Thakkar, “2001 Bhuj-Kachchh earthquake: Surface faulting and its relation with neotectonics and regional structures, Gujarat, Western India,” *Annals of Geo-Physics*, vol. 46, no. 5, pp. 937–956, 2003.
- [23] S. A. Freeman, “Response spectra as a useful design and analysis tool for practicing structural engineers,” *ASET Journal of Earthquake Technology*, vol. 44, no. 1, pp. 25–37, 2007.
- [24] K. Kasai and B. F. Maison, “Building pounding damage during the 1989 Loma Prieta earthquake,” *Engineering Structures*, vol. 19, no. 3, pp. 195–207, 1997.
- [25] S. M. Khatami, H. Naderpour, A. Mortezaei, S. T. Tafreshi, A. Jakubczyk-Galczyńska, and R. Jankowski, “Predicting the peak structural displacement preventing pounding of buildings during earthquakes,” *Journal of Physics: Conference Series*, ICAPSM, 2010, doi: 10.1088/1742-6596/2070/1/012010.
- [26] H. Naderpour, S. M. Khatami, and R. C. Barros, “Prediction of critical distance between two MDOF systems subjected to seismic excitation in terms of artificial neural networks” *Periodica Polytechnica Civil Engineering*, vol. 61, no. 3, pp. 516–529, 2017.
- [27] J. Penzien, “Evaluation of building separation distance required to prevent pounding during strong earthquakes,” *Earthquake Engineering and Structural Dynamics*, vol. 26, no. 8, pp. 849–858, 1997.
- [28] J. Lin and C. Weng, “Probability analysis of seismic pounding of adjacent buildings,” *Earthquake Engineering and Structural Dynamics*, vol. 30,

- no. 10, pp. 1539–1557, 2001.
- [29] D. Lopez-Garcia and T. T. Soong, “Evaluation of current criteria in predicting the separation necessary to prevent seismic pounding between nonlinear hysteretic structural systems,” *Engineering Structures*, vol. 31, no. 5, pp. 1217–1229, 2009.
- [30] H. Naderpour, R. C. Barros, S. M. Khatami, and R. Jankowski, “Numerical study on pounding between two adjacent buildings under earthquake excitation,” *Shock and Vibration*, vol. 2016, Art. no. 1504783.
- [31] K. Kasai, A. R. Jagiasi, and V. Jeng, “Inelastic vibration phase theory for seismic pounding mitigation,” *Journal of Structural Engineering*, vol. 122, no. 10, pp. 1136–1146, 1996.
- [32] S. M. Khatami, H. Naderpour, S. M. N. Razavi, R. C. Barros, B. Soltysik, and R. Jankowski, “An ANN-based approach for prediction of sufficient seismic gap between adjacent buildings prone to earthquake-induced pounding,” *Applied Science*, vol. 10, no. 10, 2020, Art. no. 3591.
- [33] Q. Wu, Z. Liu, T. Wang, and X. Chen, “Theoretical and experimental study of the pounding response for adjacent inelastic MDOF structures based on dimensional analysis,” *Hindawi Shock and Vibration*, vol. 2021, 2021, Art. no. 6801821.
- [34] C. Rajaram and P. K. Ramancharla, “Comparison of codal provisions on pounding between adjacent buildings,” *International Journal of Earth Sciences and Engineering*, vol. 5, no. 1, pp. 72–82, 2012.
- [35] C. Rajaram and P. K. Ramancharla, “Calculation of separation distance between adjacent buildings: A review on codal provisions,” *International Journal of Earth Sciences and Engineering*, vol. 17, no. 1, pp. 31–42, 2015.
- [36] A. K. Chopra, *Dynamics of Structures, Theory and Application to Earthquake Engineering*. New Jersey: Prentice-Hall, 1995.
- [37] M. Paz, *Structural Dynamics, Theory and Computation*. New Delhi: CBS, 1987.
- [38] *Indian standard criteria for earthquake resistant design of structures - part 1 general provisions and buildings*, IS 1893(Part 1), Bureau of Indian Standards, India, 2002.
- [39] *Indian standard ductile detailing of reinforced concrete structures subjected to seismic forces*, IS 13920, Bureau of Indian Standards, India, 1993.
- [40] *Indian standard plain and reinforced concrete*, IS 456, Bureau of Indian Standards, India, 2000.
- [41] B. Young, “Burj Khalifa Engineering the World’s Tallest Building Part 1,” Skidmore, Owings and Merrill LLP, Illinois, USA, 2022.
- [42] A. Ahmad, “Validating the structural behavior and response of Burj Khalifa: Synopsis of the full scale structural health monitoring programs,” *International Journal of High-Rise Buildings*, vol. 1, no. 1, pp. 37–51, 2012.
- [43] N. Subramanian, “Burj Khalifa, World’s Tallest Structure,” NBM and CW, vol. 15, Jan 2010.
- [44] D. S. R. Prasad, “Burj Khalifa - Construction and quality control,” *International Journal of Research in Engineering and Technology*, vol. 5, no. 20, pp. 9–19, 2016.
- [45] T. H. Setiawan, S. P. Waluyo, and N. Samudra, “The effects of façade design change on the heating and airflow through the building skin of Universitas Multimedia Nusantara Tower 3,” *Applied Science and Engineering Progress*, vol. 13, no. 2, pp. 166–174, 2020, doi: 10.14416/j.asep.2020.01.008.
- [46] A. Ahmad, S. E. K. Kim, and J. H. Kim, “Brief on the construction planning of the Burj Khalifa Project, Dubai, UAE,” presented at CTBUH, 8th World Congress, Dubai, Mar. 3–5, 2008.
- [47] W. F. Baker, D. S. Korista, and L. C. Novak, “Burj Dubai: Engineering the world’s tallest building,” *The Structural Design of Tall and Special Buildings Wiley Interscience*, vol. 16, pp. 361–375, Nov. 2007.
- [48] MATLAB, MATLAB R2022b, MathWorks, GITAM University, Visakhapatnam, India, 2022.